

VI. DIFFUSION STUDIES

A model for matrix and fracture flow regimes in unsaturated, fractured porous media at Yucca Mountain was developed by Nitao (1991). This model provides a framework for assessment of the importance of matrix diffusion at Yucca Mountain. Solute transport in fractured rock in a potential radionuclide waste repository has been discussed by Neretnieks (1990) who concluded that most rocks (even dense rocks such as granites) have small fissures between the crystals that interconnect the pore system containing water. Small molecules of radioactive materials can diffuse in and out of this pore system. The inner surfaces in the rock matrix are much larger than the surfaces in the fractures on which the water flows. The volume of water in the microfissures is much larger than the volume in fractures. Therefore, over a long time scale, diffusion can play an important role in radionuclide retardation.

The objective of our diffusion experiments was to provide diffusion information for nonsorbing neutral molecules and anions and sorbing radionuclides. Because the uptake of radionuclides by tuff is measured as a function of time, the experiments also yield information on kinetics of sorption.

A. ROCK-BEAKER EXPERIMENTS

Experimental Procedure

The experimental technique we used involved fabricating rock beakers of tuff. The beaker sits inside a Plexiglas™ container surrounded by groundwater (Fig. 128). A stopper is used to prevent evaporation. The cavity in the rock beaker has a radius of approximately 1.4 cm and a length of 2.5 cm. The beaker itself has a length of approximately 5 cm and a radius of 3.1 cm.

The radionuclides we used in these experiments were ^3H , $^{95\text{m}}\text{Tc}$, ^{237}Np , ^{241}Am , ^{85}Sr , ^{137}Cs , and ^{133}Ba . We placed a solution (prepared with groundwater from Well J-13) containing the

radionuclide of interest in the rock cavity and then analyzed aliquots of the solution from the beaker for the remaining radionuclide concentration as a function of time. We also performed batch-sorption experiments with J-13 water and the tuffs under study, using the batch-sorption procedures described in the first section of Chapter IV.

Data Analysis

The results of the rock-beaker experiments were modeled using TRACRN, a three-dimensional geochemical/geophysical-model transport code (Travis and Birdsell 1991). Because the geometry of the rock beaker is complex, an analytical solution is not available for this system. The concentration

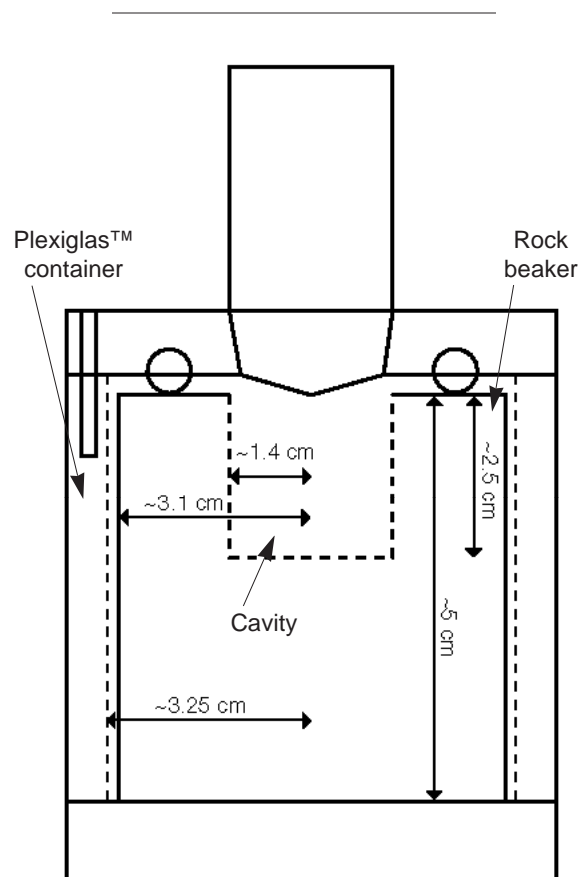


Figure 128. Rock Beaker. This cross section shows the beaker of tuff and surrounding container used in the rock-beaker diffusion experiments.

profiles of the diffusing tracer are fitted to the transport equation (de Marsily 1986, Chapter 10)

$$\nabla \cdot (\epsilon d \nabla C) = \epsilon \frac{\partial C}{\partial t} + Q, \quad (61)$$

where ϵ is the total porosity of the tuff, d is the diffusion coefficient through the tuff, C is the concentration of the diffusing tracer in solution, and the source term, Q , is zero for a nonreactive tracer but for a sorbing solute

$$Q = \rho_b \frac{\partial F}{\partial t}, \quad (62)$$

where F is the amount of tracer sorbed per unit mass of solid and ρ_b is the bulk tuff density ($\rho_b = (1 - \epsilon)\rho_s$, where ρ_s is the density of the solid particles). (Equation 41 in Chapter V reduces to the above equations for the case of no hydrodynamic dispersion, that is, the filtration velocity, \mathbf{U} , is zero and the dispersion tensor, \mathbf{D} , only includes molecular diffusion.)

As discussed in previous chapters, the mechanism of sorption determines the relationship between F and C . When sorption is linear, reversible, and instantaneous, the relationship between F and C is given by the sorption distribution coefficient

$$K_d = \frac{F}{C}. \quad (63)$$

Substitution of this equation and Eqn. 62 into Eqn. 61 yields

$$\nabla \cdot (\epsilon d \nabla C) = \epsilon R_f \frac{\partial C}{\partial t}, \quad (64)$$

where, once again, the retardation factor, R_f , is given by

$$R_f = 1 + \frac{\rho_b}{\epsilon} K_d. \quad (65)$$

Equation 65 provides a means of comparing results for sorption coefficients obtained under diffusive conditions with sorption coefficients obtained from batch-sorption experiments and is valid only if sorption is linear, reversible, and instantaneous (the Langmuir and the Freundlich isotherms are exam-

ples of nonlinear relationships between F and C). Consequently, we can determine the diffusion coefficient by fitting concentration profiles for the non-sorbing tracers, and we can determine sorption parameters, such as K_d , by fitting concentration profiles for the sorbing tracers.

Results and Discussion

Figure 129 shows an example of a set of diffusion data for a rock-beaker experiments in which we used the feldspar-rich tuff G4-737 and solutions of tracers in J-13 water. The concentration of tracer, C , remaining in the solution inside the cavity of the rock beaker divided by the initial concentration, C_o , is plotted as a function of elapsed time.

The solid lines in Fig. 130 are a fit of these same data to the diffusion equation (Eqn. 61) using the TRACRN transport code for the two nonsorbing radionuclides, tritium and technetium-95m. The diffusion coefficients obtained in this manner for these radionuclides for all the tuff samples studied (Table 33) agree well with previous results (Rundberg et al. 1987). These two tracers diffuse essentially as tritiated water and the pertechnetate anion, TcO_4^- . Large anions are excluded from tuff pores because of their size and charge, which can account for the lower diffusivity of TcO_4^- .

If sorption is linear, reversible, and instantaneous, then F/C is equal to a sorption coefficient, K_d . To test this assumption, we determined values of K_d in batch-sorption experiments using the tuffs under study (Table 34). We then calculated an expected diffusion curve using, for each tuff, the diffusion coefficient measured for tritiated water and the batch-sorption coefficient measured for each sorbing radionuclide. Figure 131 shows these calculated diffusion curves for tuff G4-737. Comparison of the calculated curves with the actual measured data (see the example in Fig. 132) shows that the concentration of the sorbing radionuclides remaining in the rock beaker drops faster than predicted on the basis of a linear K_d . This result indicates that the diffusion of the sorbing radionuclides

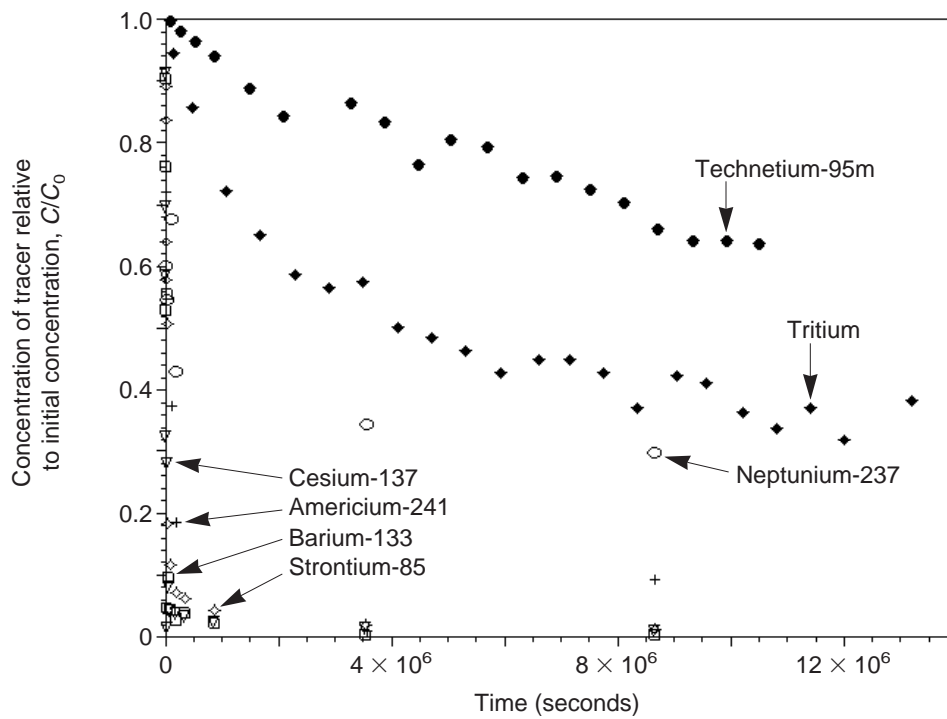


Figure 129. Diffusion Data. These data for diffusion of tracers in J-13 water and in rock beakers made of tuff G4-737 show the concentration, C , of tracer (relative to the initial concentration, C_0) remaining in the beaker as a function of elapsed time.

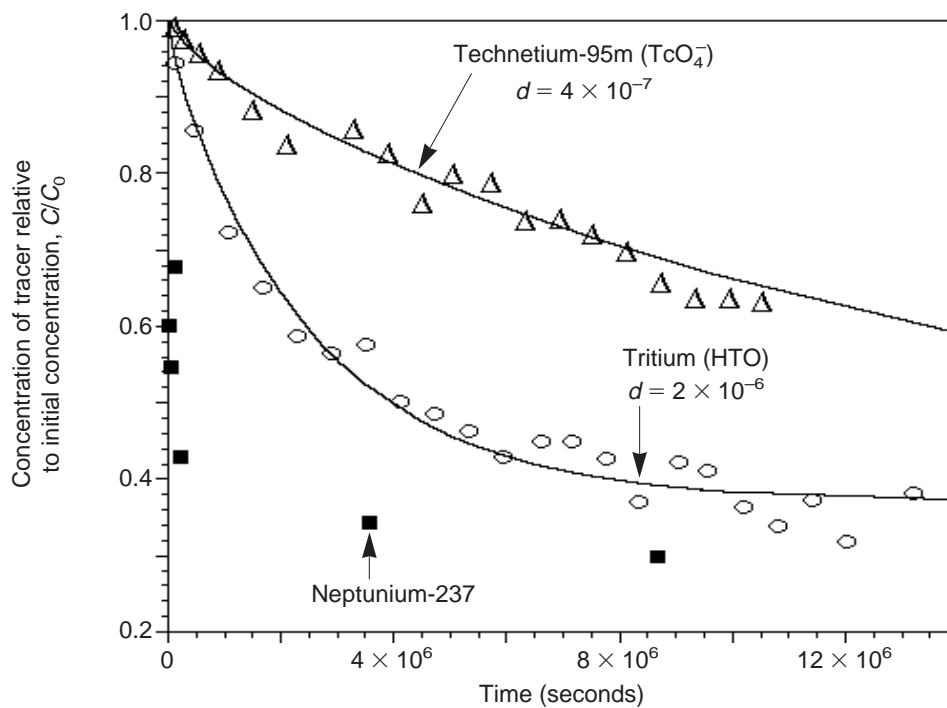


Figure 130. Diffusion Data Curve Fits. The solid curves are fits to the diffusion data by the TRACRN code for the nonsorbing tracers tritium and technetium in the rock-beaker experiments with tuff G4-737.

Table 33. Rock-beaker Diffusion Results for Nonsorbing Radioisotopes

Tuff sample	Major minerals	Porosity	Diffusion coefficient, d (cm ² /s)	
			HTO	TcO ₄ ⁻
G4-737	Alkali feldspar 68% Cristobalite 28%	0.07	2.2×10^{-6}	3.9×10^{-7}
GU3-304 #1	Alkali feldspar 75%	0.06	1.5×10^{-6}	3.0×10^{-7}
GU3-304 #2	Cristobalite 25%		1.6×10^{-6}	3.0×10^{-7}
GU3-433	Alkali feldspar 76% Cristobalite 15%	0.10	3.5×10^{-6}	
GU3-1119	Alkali feldspar 70% Quartz 19%	0.10	2.0×10^{-6}	4.9×10^{-7}
Topopah outcrop	Alkali feldspar 59% Cristobalite 23% Quartz 12%	0.07	1.0×10^{-6}	1.0×10^{-7}

Table 34. Batch-sorption Diffusion Coefficients

Tuff sample	Major minerals	Diffusion coefficient, K_d (ml/g)				
		Neptunium	Americium	Cesium	Strontium	Barium
G4-737	Alkali feldspar 68% Cristobalite 28%	8	134	532	52	28
GU3-304	Alkali feldspar 75% Cristobalite 25%	8		342	18	19
GU3-433	Alkali feldspar 76% Cristobalite 15%	9	154	1264	20	61
GU3-1119	Alkali feldspar 70% Quartz 19%	8	136	494	42	27
Topopah outcrop	Alkali feldspar 59% Cristobalite 23% Quartz 12%	9		465	20	25

could not be fitted by assuming reversible, instantaneous, and linear sorption. These results also indicate that transport calculations using a batch-sorption K_d value and the diffusion coefficient measured for tritiated water will result in conservative predictions for the transport of sorbing

radionuclides.

The results obtained from rock-beaker experiments agree with previous results (Rundberg 1987). We performed experiments on the uptake of sorbing radionuclides by tuff and found that

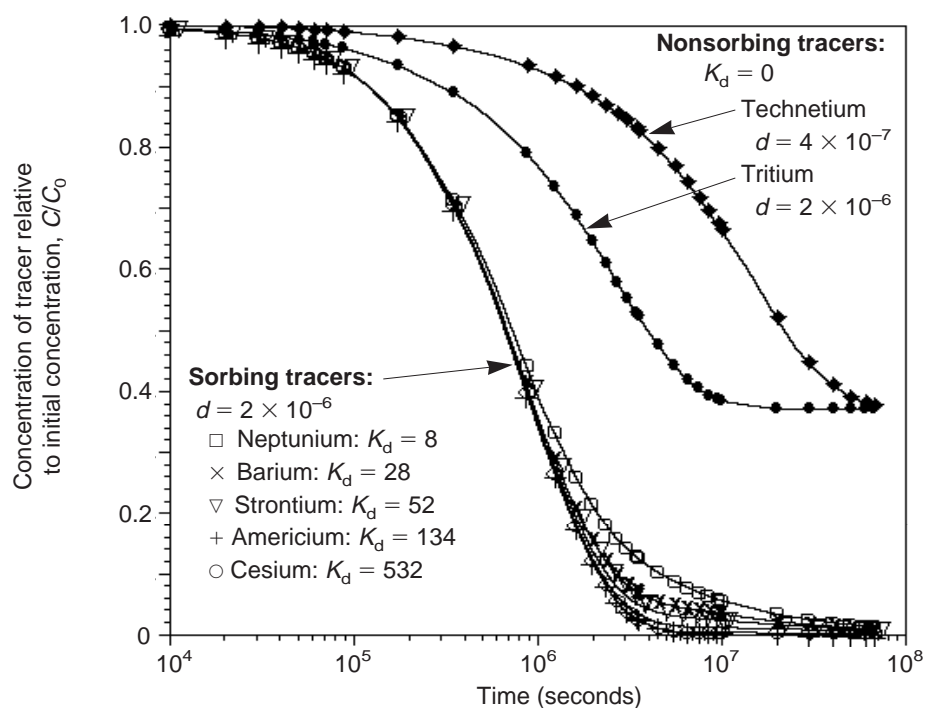


Figure 131. Calculated Diffusion Curves. These curves were calculated for tuff G4-737 using the diffusion coefficient, d , measured for tritiated water and the batch-sorption coefficients, K_d , measured for the sorbing radionuclides (given in Table 34). The diffusion curves for tritium and technetium are also shown.

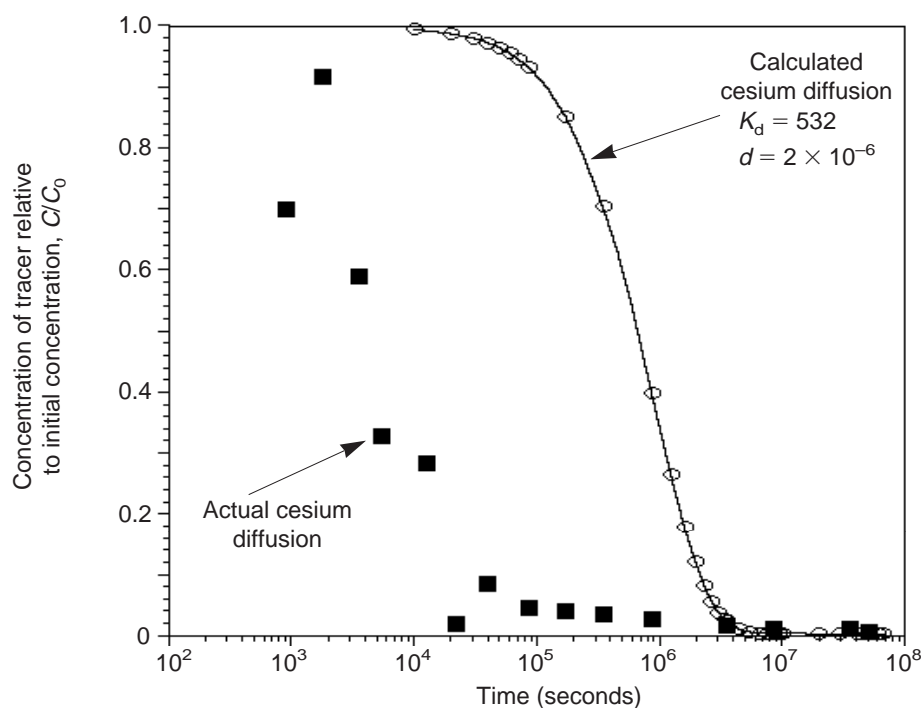


Figure 132. Comparison of Calculated and Actual Diffusion Data. The solid curve is the diffusion curve calculated for cesium using a K_d value and the diffusion coefficient for tritium (Fig. 131); the squares are the actual diffusion data for cesium with tuff G4-737 (Fig. 129).

rate constants for uptake of the sorbing cations from solution onto tuff were consistent with a diffusion-limited model in which diffusion occurs in two stages. In the first stage, the cations diffuse into rock through water-filled pores; in the second stage, they diffuse into narrower intracrystalline channels. This diffusion model yielded sorption coefficients for cesium, strontium, and barium that agree well with the sorption coefficients determined by batch techniques.